Enhanced microwave absorption properties of Y-doped $LaMnO_3$ prepared by a solid state reaction method

WEIHONG MA*, QUANXI CAO, BO WANG, ZI YANG, TAIPENG ZHOU, QUN ZHAO
School of Advanced Materials and Nanotechnology, Xidian University, Xi'an, Shaanxi 710126, China

Y-doped $LaMnO_3$ powders with doping ratios of 5%, 10%, and 15% were prepared by a solid state reaction method and tested as microwave absorption material. X-ray diffraction measuring results indicated that the powders possess a perovskite structure at all doping ratios. The average size of the powders was approximately 3μm according to scanning electron microscopy. The complex permittivity and permeability were measured at X-band (8.2–12.4GHz) by a vector network analyzer. The dielectric loss tangent ($\tan\delta_\varepsilon$), magnetic loss tangent ($\tan\delta_\mu$), and reflectivity–frequency curves are presented. 10at% Y-doped $LaMnO_3$ with a thickness of 0.8mm had an effective -10dB bandwidth of 3GHz, and the highest absorption peak (-45dB); this is comparable to the characteristics of other advanced manganate-based microwave absorption materials.

(Received March 21, 2015; accepted April 5, 2016)

Keywords: Y-doped $LaMnO_3$, Microwave absorption material, Electromagnetic loss

1. Introduction

Stealth and electromagnetic compatibility (EMC) technologies are becoming increasingly important; electromagnetic wave absorbing materials have become indispensable, and are regarded as a "secret weapon" in modern military electronic warfare [1]. These materials play a prominent role in military stealth technology, anechoic chamber construction, and security systems [2-3]. Meanwhile, with the development of modern science and technology, the impact of electromagnetic radiation on normal life is also increasing: commercial aircraft schedules can be disrupted by electromagnetic interference, and hospital medical equipment can malfunction because of mobile phone interference. Therefore, absorbing materials have become essential for both national defense and civilian technologies. Domestic and foreign researchers are currently working not only to improve traditional absorbing materials, but also to develop new types of such materials [4]. A transition metal oxide, doped with a rare-earth that produces giant magnetoresistance has become a research focus for application as absorbing materials [5-8]. Doped $LaMnO_3$ is a typical giant magnetoresistive material. Li et al. [9] and Hu et al. [10] studied the microwave absorption characteristics of $La_xSr_{1-x}MnO_3$ within the frequency range of 8–12 GHz. They found that the absorption bandwidth for a reflection loss (R) greater than -8 dB was 3 GHz, and the absorption peak height was -25 dB.

It is well-known that Y-doping causes variations at the A-sites of the perovskite lattice. Changes in the lattice parameter and structure cause an increase in the internal stress, which is attributed to the smaller ionic radius, larger electronegativity and non-uniform distribution of the Y ion. The increased internal stress results in the localization of the carriers due to the enhanced Mn-O-Mn chemical bond; this reduces the resistivity and increases the dielectric loss of the sample to a certain extent. Furthermore, disorder of Mn ions is caused by the enhanced tortuosity of the Mn-O-Mn chemical bond. Under an applied magnetic field, the crystal structure changes from low symmetry to high symmetry and the ordering transforms from anti-ferromagnetism to ferromagnetism, which increases the magnetic losses [7].

In this study, powdered manganese oxides, $La_xY_{1-x}MnO_3$, were fabricated by solid state reaction and were doped by substituting the rare earth yttrium in some of the A-site positions; the electromagnetic characteristics and the microwave-absorbing behavior of this material were explored. The results indicated that, when the thickness of $La_{0.9}Y_{0.1}MnO_3$ was 0.8 mm, the effective absorption bandwidth for R < -10 dB was as high as 3 GHz within the frequency range of 8.2–12.4 GHz. This composition provided a wider effective absorption band and higher absorption coefficient than other materials.

2. Experiment

$La_{1-x}Y_xMnO_3$ powders (x = 0, 0.05, 0.1, 0.15) were synthesized by a standard solid state reaction method. Analytically pure La_2O_3, $MnCO_3$ and Y_2O_3, purchased from Shanghai Chemical Reagent Co. and Tianjin Fuchen Chemical Reagent Factory were used as the raw materials. The powders were mixed in a stoichiometric ratio and milled in a planetary ball mill at 300 rpm for 5h, with ethanol as the milling medium. The mixed slurry was

placed in a drying box at 80 °C for 12 h, then the materials were milled through a 60 mesh sieve and sintered in an air atmosphere at 1300 °C for 4h. Finally, the materials were milled again through a 60 mesh sieve to produce $La_{1-x}Y_xMnO_3$ powders.

The crystal structure of the samples was characterized by X-ray diffraction (XRD) using a Cu target at a working voltage and current of 35 kV and 25 mA, respectively. The powders were characterized by scanning electron microscopy (SEM) to determine the particle size and morphology. Composite specimens for the measurement of the electromagnetic parameters were prepared by mixing the $La_{1-x}Y_xMnO_3$ powders with paraffin in a weight ratio of 1:1, and the electromagnetic parameters (complex permittivity, $\varepsilon = \varepsilon' - j\varepsilon''$ and complex permeability, $\mu = \mu' - j\mu''$) of the samples were measured at various microwave frequencies in the range of 8.2–12.4 GHz, using a microwave vector network analyzer. The reflectivity loss R was calculated at different frequencies by MATLAB, using the measured values for the electromagnetic parameters.

3. Results and analysis

3.1 Crystal structure of the samples and particle morphology

Fig. 1 shows the XRD pattern of $La_{1-x}Y_xMnO_3$ (x = 0, 0.05, 0.1, 0.15) powders, which were fabricated with different amounts of Y and sintered at 1300 °C. As can be seen from the figure, the perovskite structure was formed despite the introduction of Y^{3+}; the $LaMnO_3$ and $La_{0.9}Y_{0.1}MnO_3$ samples had a well-defined single phase. The X-ray diffraction peak of the Y-doped samples (x = 0.05, x = 0.1, x = 0.15) was higher, clearer, and sharper, than the peak of the undoped sample (x = 0). A possible explanation is that the Y_2O_3 helped promote the synthesis of $LaMnO_3$ by acting as a flux. However, because of the limit of the solution line, there is no impurity peak while x = 0.1, i.e. the phase of the $La_{0.9}Y_{0.1}MnO_3$ sample was in good agreement with the $LaMnO_3$ sample.

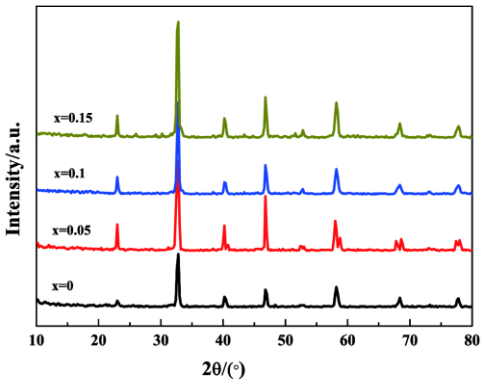

Fig. 1. XRD pattern of $La_{1-x}Y_xMnO_3$ (x = 0, 0.05, 0.1, 0.15) powders sintered at1300 °C

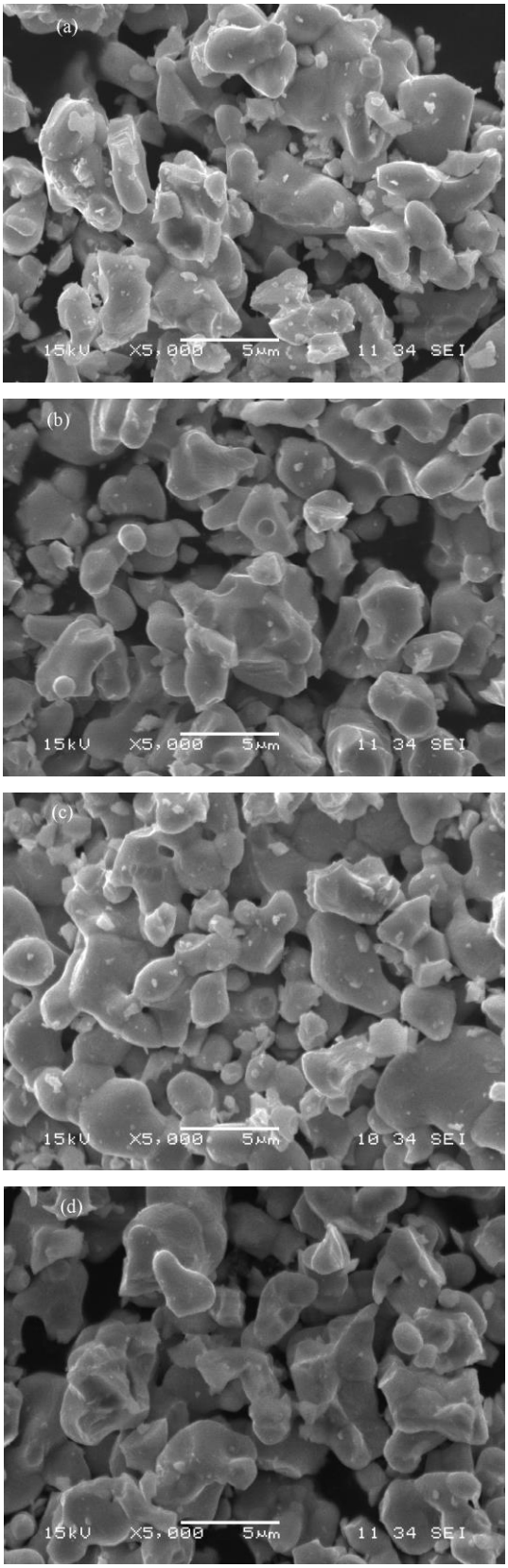

Fig. 2. SEM photographs of four samples of the $La_{1-x}Y_xMnO_3$ powder. (a) x = 0 ; (b) x = 0.05 ; (c) x = 1 ; (d) x = 0.15

Fig. 2 shows the morphologies of $La_{1-x}Y_xMnO_3$

powders with different concentrations of Y^{3+}; typical grain size was approximately 3 μm, and it is notable that the powders exhibited good dispersion, similar morphology, and homogeneous grain size. There was melting at the edges of the grains to an extent due to the introduction of Y^{3+} that formed a solid solution of $La_{1-x}Y_xMnO_3$. The degree of melting increased with the amount of Y^{3+}.

3.2 Dielectric and magnetic parameters

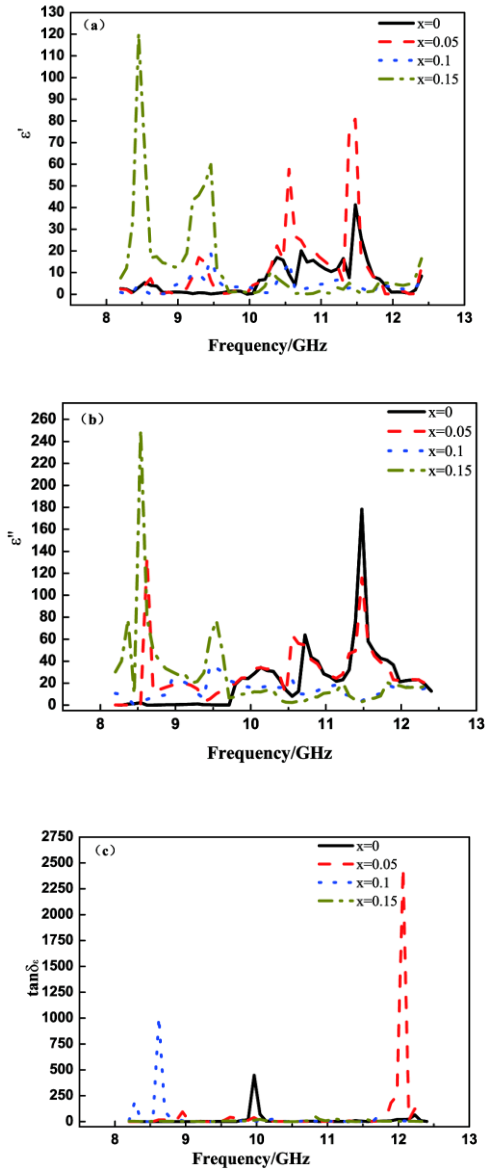

Fig. 3. Permittivity of the prepared powders with different Y^{3+} content. (a) ε', the real part of dielectric constant; (b) ε'', the imaginary part of the dielectric constant; (c) tan δ_ε, the electrical loss tangent

Fig. 3 shows the permittivity of $La_{1-x}Y_xMnO_3$ powders (x = 0, 0.05, 0.1, 0.15) in the frequency range of 8.2–12.4 GHz. As shown in the figures, for a given value of x, the real and imaginary parts of the permittivity followed roughly the same trend as the frequency was varied. Moreover, the imaginary part was larger than the real part. For x = 0.05, the imaginary part had a peak in the vicinity of 8.6 GHz. For x = 0.1, the values of the real and imaginary parts were smaller than those for the other samples. As x increased, the real part of the permittivity increased gradually within the frequency range of 8.2–10.0 GHz, but over the same range, the imaginary part first increased, then decreased, and finally increased again. In the frequency range of 10.0–12.4 GHz, the real part of the permittivity first increased and then decreased, while the imaginary part decreased gradually. In Fig. 3(c), it can be seen that when x = 0.1, the electric loss tangent had a fairly high peak, and when x = 0.05, it had its maximum peak. For x = 0.15, the electric loss tangent did not have any peaks.

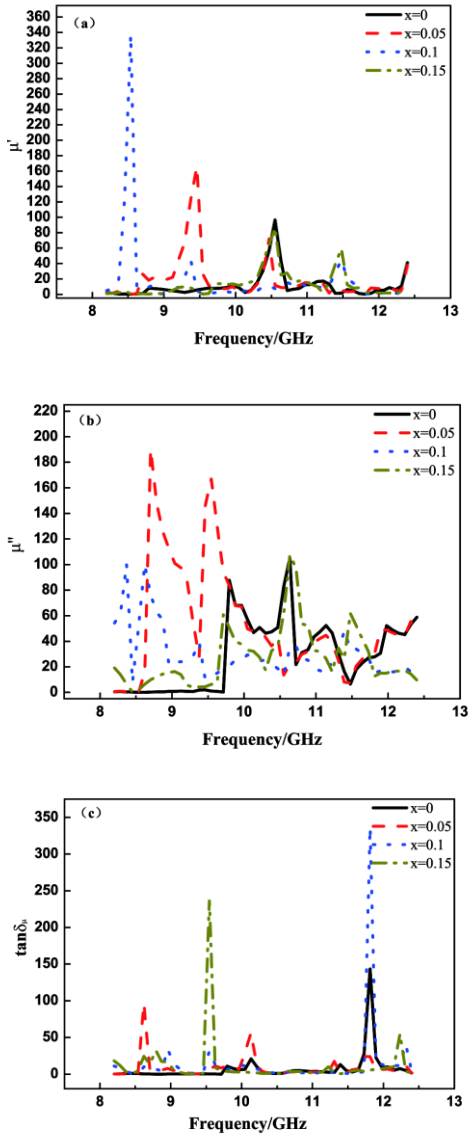

Fig. 4. Magnetic permeability of the prepared powders with different Y content. (a) μ', the real part of the permeability; (b) μ'', the imaginary part of the permeability; (c) tan δ_μ, the magnetic loss tangent

Fig. 4 shows the magnetic permeability of $La_{1-x}Y_xMnO_3$ powders (x = 0, 0.05, 0.1, 0.15) in the frequency range of 8.2–12.4 GHz. It can be seen in Fig. 4(a) that the peak of the real part of the permeability moves first to a low frequency, and then towards a high frequency, as x increases; then, the peak first increased and then decreased. Fig. 4(b) shows the imaginary part of the permeability μ''. The peak of μ'' has the same trend as that of μ'; but for each sample, the imaginary part of the permeability has two large peaks at slightly separated frequencies, compared to a single peak in the case of the real part. Fig. 4(c) shows that the magnetic loss tangent had a high peak when x = 0.1 and 0.15, but a small peak when x = 0.05. Comparing Fig. 3 and Fig. 4, it can be seen that the frequency of each ε peak was different from that of the corresponding μ peak for all the different values of x.

Comparing Fig. 3(c) and Fig. 4(c), it can be noted that when x = 0.05, the electrical loss tangent had a maximum peak, but the peak of the magnetic loss tangent was small. When x = 0.15, the magnetic loss tangent had a high peak, but the electric loss tangent did not have any peaks. When x = 0.1, both the electrical loss tangent and the magnetic loss tangent had large peaks; therefore, the sample with x = 0.1 should have the best microwave absorption properties.

Y^{3+} addition could promote the presence of ferromagnetic and form antiferromagnetic clusters simultaneously [11-13]. The peaks of the magnetic loss factor, tan δ_μ, are formed by the natural resonance of the ferromagnetic cluster while the peaks of the dielectric loss factor, tan δ_ε, are formed because the dielectric dipole orientation polarization causes electrical relaxation [14] of the antiferromagnetic cluster.

3.3 Microwave reflection properties

A non-zero R implies microwave absorption properties. According to transmission line theory [15], the normalized input impedance Z_{in} of a metal-backed microwave absorbing layer is given by:

$$Z_{in} = (\mu/\varepsilon)^{1/2}\tanh(j2\pi fd(\mu\varepsilon)^{1/2}/c), \quad (1)$$

where μ and ε are the relative complex permeability and permittivity, respectively, of the composite, c is the velocity of light, d is the thickness of the monolayer absorber, and f is the frequency.

R can be obtained from the following equation:

$$R = 20\log|(Z_{in}-1)/(Z_{in}+1)| \quad (2)$$

The reflection loss of the composite medium is determined by six parameters: the real and imaginary parts of the relative complex permittivity ($\varepsilon = \varepsilon' - j\varepsilon''$) and permeability ($\mu = \mu' - j\mu''$), the thickness of the absorber, and the working frequency.

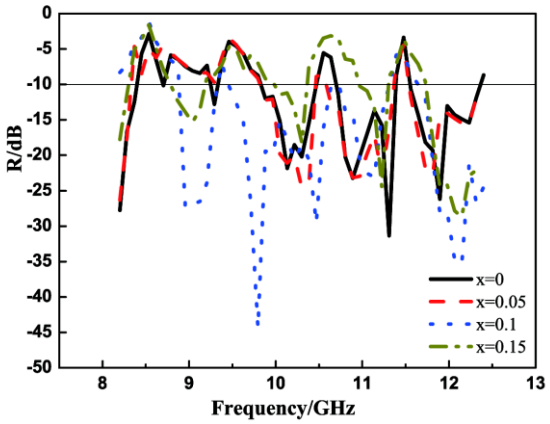

Fig. 5. Reflectivity of a $La_{1-x}Y_xMnO_3$ (x = 0, 0.05, 0.1, 0.15) sheet with a thickness of 0.8 mm

The reflection loss of $La_{1-x}Y_xMnO_3$ (x = 0, 0.05, 0.1, 0.15) samples were investigated using equation (2). Fig. 5 shows the reflectivity of $La_{1-x}Y_xMnO_3$ (x = 0, 0.05, 0.1, 0.15) with a thickness of 0.8 mm; and Table 1 shows the minimum reflection loss, R < -10 dB absorption bandwidth, and matching frequency. The microwave absorbing peak initially shifted to lower frequencies after Y-doping in comparison with that of undoped $LaMnO_3$, and then rose again for x = 0.15; the effective absorption band for R < -10dB first widened and then narrowed again. When x = 0.1, the effective microwave absorption band was the widest and the absorption peak was the highest.

Table 1. Microwave absorption properties of $La_{1-x}Y_xMnO_3$ (x = 0, 0.05, 0.1, 0.15) with a thickness of 0.8 mm

Samples	R < -10 dB absorbing bandwidth(*GHz*)	Matching frequency(*GHz*)	Maximum reflection loss(*dB*)
$LaMnO_3$	2.0	11.30	-31.46
5at% Y- $LaMnO_3$	2.0	10.30	-24.39
10at%Y-$LaMnO_3$	3.0	9.79	-45.00
15at%Y-$LaMnO_3$	1.8	12.20	-28.77

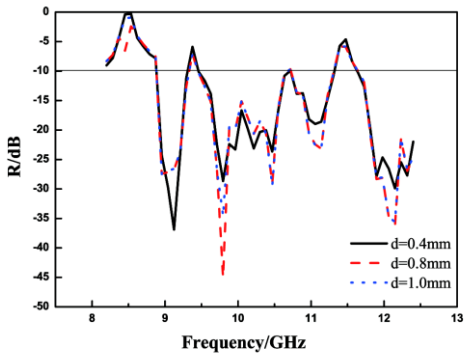

Fig. 6. The reflectivity of $La_{0.9}Y_{0.1}MnO_3$ powders of different thicknesses (d)

Fig. 6 presents the reflectance of $La_{0.9}Y_{0.1}MnO_3$ powders of different thicknesses (*d*); the -10 dB bandwidth did not change significantly as a function of layer thickness. Table 2 shows the microwave absorbing properties of $La_{0.9}Y_{0.1}MnO_3$ as a function of thickness; when the thickness was 0.8 mm, the absorption peak reached its maximum value of -45 dB. Thus, the optimum thickness for a $La_{0.9}Y_{0.1}MnO_3$ powder absorber was about 0.8 mm.

Table 2. Microwave absorption properties of $La_{0.9}Y_{0.1}MnO_3$ powders of different thicknesses (d)

Samples	Thickness(*mm*)	*R* < -10 dB absorbing bandwidth(*GHz*)	Matching frequency(*GHz*)	Maximum reflection loss(*dB*)
$La_{0.9}Y_{0.1}MnO_3$	0.4	3.0	9.12	-36.89
	0.8	3.0	9.79	-45.00
	1.0	3.0	12.15	-35.58

4. Conclusion

1. $La_{1-x}Y_xMnO_3$ microwave-absorbing powder, at 4 doping levels, was fabricated successfully by a solid-state reaction method in an air atmosphere, by sintering at 1300 °C for 4 h.
2. When the thickness was 0.8 mm, $La_{0.9}Y_{0.1}MnO_3$ was a strong and wideband microwave absorbing material within the frequency range of 8.2–12.4 GHz,. The effective absorption bandwidth for *R* < -10 dB was 3 GHz and the maximum absorption peak was -45 dB. Hence, this material could be valuable as a microwave absorbing material.
3. The peak values of the electric and magnetic loss tangents of $La_{0.9}Y_{0.1}MnO_3$ were relatively large. The reflection loss of this material came from the combined effect of dielectric loss and magnetic loss. As the microwave frequency was changed, the dielectric loss and magnetic loss varied in opposite directions to each other. This may have been caused by the transition between ferromagnetic and antiferromagnetic clusters.

References

[1] Z. B. Li, B. Shen, Y. D. Deng, L. Liu, W. B. Hu, Applied Surface Science, **255**, 4542 (2005).
[2] Y. B. Feng, T. Qiu, C. Y. Shen, Journal of Magnetism and Magnetic Materials, **318,** 8 (2007).
[3] X. M. Shen, L. S. Li, X. R. Wu, Z. F. Gao, G. Y. Xu, Journal of Alloys and Compounds, **509,** 8116 (2011).
[4] B. Wang, Q. X. Cao, S. Y. Zhang, Materials Science in Semiconductor Processing, **19,** 101 (2014).
[5] F. X. Hu, J. Gao, X. S. Wu, Physical Review B, **72,** 1 (2005).
[6] S. Okuyuma, K. Takenaka, R. Shiozaki, Physica B, **329-333,** 846 (2003).
[7] D. S. Dai, G. C. Xiong, S. C. Wu, Progress in Physics, **17,** 201 (1997).
[8] N. Tomohiko, U. Yutaka, Journal of Alloys and Compounds, **383,** 135 (2004).
[9] G. Li, G. G. Hu, H. D. Zhou, Materials Chemistry and Physics, **75,** 101 (2002).
[10] G. G. Hu, P. Yin, Q. R. Li, Chinese Rare Earths, **20,** 179 (2002).
[11] U. Topal, C. Birlikseven, M. E. Yakınci, T. Nurgaliev, Journal of Alloys and Compounds, **492,** 8 (2010).
[12] A. Kirilyuk, K. Demyk, G. V. Helden, Journal of Applied Physics, **93** 7379 (2003).
[13] Y. K. Tang, X. Ma, Z. Q. Kou, Physical Review B, **72,** 1 (2005).
[14] S .Y. Zhang, Q. X. Cao, X. H. Ma, Z. M. Li, Applied Surface Science, **258,** 7036 (2012).
[15] S. Y. Zhang, Q. X. Cao, Materials Science and Engineering B **177,** 678 (2012).

*Corresponding author: weihongma@xidian.edu.cn